

Stimuli-Responsive Disassembly of Nanoparticle Aggregates for Light-Up Colorimetric Sensing

Juewen Liu and Yi Lu*

Contribution from the Department of Chemistry and Beckman Institute for Advanced Science and Technology, University of Illinois at Urbana-Champaign, Urbana, Illinois, 61801

Received June 1, 2005; E-mail: yi-lu@uiuc.edu

Abstract: Controlled assembly of nanomaterials has been the focus of much research. In contrast, controlled disassembly has not received much attention, even though both processes have been shown to be important in biology. By using a Pb^{2+} -dependent RNA-cleaving DNAzyme, we demonstrate here control of the disassembly of gold nanoparticle aggregates in response to Pb^{2+} . In the process, we show that nanoparticle alignment plays an important role in the disassembly process, with the tail-to-tail configuration being the most optimal, probably because of the large steric hindrance of other configurations. The rate of disassembly is significantly accelerated by using small pieces of DNA to invade the cleaved substrate of the DNAzyme. Investigation of such a controlled disassembly process allows the transformation of previously designed "light-down" colorimetric Pb^{2+} sensors into "light-up" sensors.

Introduction

Controlled synthesis and properties of materials in response to chemical stimuli is a hallmark of biology. Employing such a process in nanoscale science and engineering can result in novel materials that rival or even exceed the structure and function of naturally occurring materials. Toward this goal, DNA has been used as an ideal programmable template to assemble materials with high controllability.^{1–3} For example, DNA-functionalized nanoparticles have been assembled into dimer/trimer^{4,5} or aggregates^{6,7} with complementary DNA. The latter process was further developed as a simple and highly sensitive colorimetric detection method for sequence-selective sensing of DNA.⁸ Another useful feature of DNA is that it can be programmed to form unique topological and geometric structures,⁹ such as knots,¹⁰ cubes,¹¹ truncated octahedrons,¹² and octahedrons.¹³ DNA can also be constructed into periodic one-, two-, and three-dimensional structures, upon which nanoparticles or proteins can be deposited to form well-defined patterns.^{14–17}

In addition to precisely programmed material synthesis, biology often exerts additional controls so that a thermodynamically favorable process will not occur in the absence of a chemical stimulus that triggers the process. A recent example is the discovery of riboswitches that control mRNA translation to protein synthesis by the presence of certain metabolites.¹⁸ To apply the biological concept of controlled materials synthesis in response to chemical stimuli, we employed catalytic DNA molecules (DNAzymes)^{19–24} whose activities depend specifically on cofactors such as metal ions or organic molecules to assemble nanoparticles.^{25–28} Such DNAzyme/nanoparticle systems possess not only programmable structures, but also biological functions and practical applications. The Pb^{2+} -dependent DNAzyme is composed of an enzyme (17E) and a substrate strand (17DS) (Figure 1A). The substrate contains a single RNA linkage (rA) that serves as the cleavage site. In the presence of Pb^{2+} , the enzyme cleaves the substrate into two pieces (Figure 1B).^{29–32} To assemble nanoparticles, the substrate (17DS) was extended on both ends by 12 bases to be

- (1) Storhoff, J. J.; Mirkin, C. A. *Chem. Rev.* **1999**, *99*, 1849–1862.
- (2) Niemeyer, C. M. *Angew. Chem., Int. Ed.* **2001**, *40*, 4128–4158.
- (3) Katz, E.; Willner, I. *Angew. Chem., Int. Ed.* **2004**, *43*, 6042–6108.
- (4) Alivisatos, A. P.; Johnsson, K. P.; Peng, X.; Wilson, T. E.; Loweth, C. J.; Bruchez, M. P., Jr.; Schultz, P. G. *Nature* **1996**, *382*, 609–611.
- (5) Loweth, C. J.; Caldwell, W. B.; Peng, X.; Alivisatos, A. P.; Schultz, P. G. *Angew. Chem., Int. Ed.* **1999**, *38*, 1808–1812.
- (6) Mirkin, C. A.; Letsinger, R. L.; Mucic, R. C.; Storhoff, J. J. *Nature* **1996**, *382*, 607–609.
- (7) Dujardin, E.; Mann, S.; Hsin, L.-B.; Wang, C. R. C. *Chem. Commun.* **2001**, 1264–1265.
- (8) Elghanian, R.; Storhoff, J. J.; Mucic, R. C.; Letsinger, R. L.; Mirkin, C. A. *Science* **1997**, *277*, 1078–1080.
- (9) Seeman, N. C. *Curr. Opin. Struct. Biol.* **1996**, *6*, 519–526.
- (10) Du, S. M.; Stollar, B. D.; Seeman, N. C. *J. Am. Chem. Soc.* **1995**, *117*, 1194–1200.
- (11) Chen, J.; Seeman, N. C. *Nature* **1991**, *350*, 631–633.
- (12) Zhang, Y.; Seeman, N. C. *J. Am. Chem. Soc.* **1994**, *116*, 1661–1669.
- (13) Shih, W. M.; Quispe, J. D.; Joyce, G. F. *Nature* **2004**, *427*, 618–621.
- (14) Winfree, E.; Liu, F.; Wenzler, L. A.; Seeman, N. C. *Nature* **1998**, *394*, 539–544.
- (15) Xiao, S.; Liu, F.; Rosen, A. E.; Hainfeld, J. F.; Seeman, N. C.; Musier-Forsyth, K.; Kiehl, R. A. *J. Nanopart. Res.* **2002**, *4*, 313–317.

- (16) Yan, H.; Park, S. H.; Finkelstein, G.; Reif, J. H.; LaBean, T. H. *Science* **2003**, *301*, 1882–1884.
- (17) Deng, Z.; Mao, C. *Angew. Chem., Int. Ed.* **2004**, *43*, 4068–4070.
- (18) Winkler, W.; Nahvi, A.; Breaker, R. R. *Nature* **2002**, *419*, 952–956.
- (19) Joyce, G. F. *Annu. Rev. Biochem.* **2004**, *73*, 791–836.
- (20) Breaker, R. R. *Nat. Biotechnol.* **1997**, *15*, 427–431.
- (21) Breaker, R. R. *Science* **2000**, *290*, 2095–2096.
- (22) Sen, D.; Geyer, C. R. *Curr. Opin. Chem. Biol.* **1998**, *2*, 680–687.
- (23) Lu, Y. *Chem.–Eur. J.* **2002**, *8*, 4588–4596.
- (24) Achenbach, J. C.; Chiuman, W.; Cruz, R. P. G.; Li, Y. *Curr. Pharm. Biotechnol.* **2004**, *5*, 312–336.
- (25) Liu, J.; Lu, Y. *J. Am. Chem. Soc.* **2004**, *126*, 12298–12305.
- (26) Liu, J.; Lu, Y. *Chem. Mater.* **2004**, *16*, 3231–3238.
- (27) Liu, J.; Lu, Y. *J. Am. Chem. Soc.* **2003**, *125*, 6642–6643.
- (28) Liu, J.; Lu, Y. *Anal. Chem.* **2004**, *76*, 1627–1632.
- (29) Santoro, S. W.; Joyce, G. F. *Proc. Natl. Acad. Sci. U.S.A.* **1997**, *94*, 4262–4266.
- (30) Li, J.; Zheng, W.; Kwon, A. H.; Lu, Y. *Nucleic Acids Res.* **2000**, *28*, 481–488.
- (31) Brown, A. K.; Li, J.; Pavot, C. M. B.; Lu, Y. *Biochemistry* **2003**, *42*, 7152–7161.
- (32) Cruz, R. P. G.; Withers, J. B.; Li, Y. *Chem. Biol.* **2004**, *11*, 57–67.

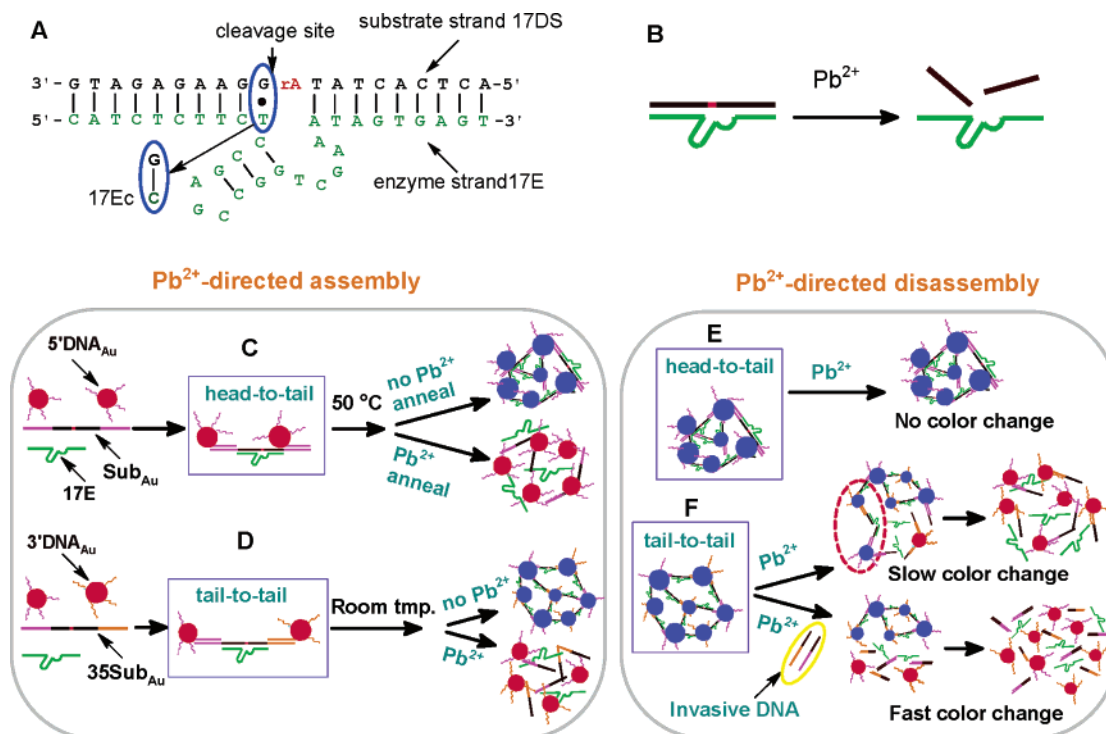


Figure 1. (A) Secondary structure of the DNAzyme. (B) Cleavage of 17DS by 17E in the presence of Pb^{2+} . Pb^{2+} -directed assembly of gold nanoparticles by the DNAzyme when nanoparticles are aligned in a head-to-tail (C) or a tail-to-tail (D) manner. (E) For head-to-tail aligned aggregates, Pb^{2+} cannot induce DNAzyme cleavage and no color change can be observed. (F) For tail-to-tail aligned aggregates, Pb^{2+} can induce DNAzyme cleavage and color change can be observed. The rate of color change can be significantly increased by adding invasive DNA.

complementary to the DNA attached to nanoparticles. The nanoparticles were aligned either in a head-to-tail manner (Figure 1C)²⁷ or in a tail-to-tail manner (Figure 1D).²⁵ In the former case, a heating-and-cooling process (annealing) was required to form nanoparticle assemblies, while in the latter case aggregates were formed at ambient temperatures. For both alignments, nanoparticle solutions changed color from red to blue upon aggregation. In the presence of Pb^{2+} , the substrate was cleaved by the enzyme, which inhibited aggregation, and the color remained red. Therefore, Pb^{2+} can direct the assembly state of nanoparticles, and colorimetric Pb^{2+} sensors were designed based on this process.

Besides controlled *assembly* of materials in response to chemical stimuli,^{6,7,33,34} biology also demonstrates control of the *disassembly* of materials in response to chemical stimuli such as controlled release of iron from iron nanoclusters in the iron storage protein ferritin.³⁵ This reverse process has not been a focus of study even though disassembly of nanomaterials could be equally or sometimes even more useful.^{8,36} For example, the sequence-selective detection of DNA reported by Mirkin and co-workers was achieved by measuring melting temperatures of nanoparticle aggregates assembled by DNA.⁸ In the melting process, nanoparticles dispersed from the aggregates. For the Pb^{2+} sensing systems reported by us,^{25–27} nanoparticles remained unassembled and the color remained red in the presence of the target analyte Pb^{2+} (Figure 1C,D). Color change to blue was observed only in the absence of Pb^{2+} . From the sensing

point of view, these are “light-down” sensors. Since such sensors rely on the absence of a color change for positive detections, they are vulnerable to environmental factors that may inhibit the color change. On the other hand, studying Pb^{2+} -induced disassembly may generate materials that can be used as “light-up” colorimetric sensors. More importantly, the system allows systematic investigation of interactions between biopolymers with inorganic nanoparticles in the assembled state. Herein we report controlled disassembly of gold nanoparticle aggregates in response to Pb^{2+} . Its application as a “light-up” colorimetric Pb^{2+} sensor is also demonstrated.

Results and Discussion

Size and Size Distribution of Nanoparticle Aggregates. To study the disassembly of nanoparticle aggregates, it is helpful to estimate the average size of an aggregate and the number of nanoparticles it contains. The size and size distribution of nanoparticle aggregates assembled by the DNAzyme were characterized by TEM (Figure 2C,D). Most aggregates were irregular in shape, and almost no free nanoparticles were observed. For statistical purposes, the longest dimension of an aggregate was used to represent its size. On the basis of the size distribution, more than 98% of nanoparticles were present in aggregates larger than 2 μm (Figure 2E). It was estimated that a 2- μm aggregate contained around 10 000 13-nm-diameter nanoparticles. The aggregates were normally prepared and suspended in a buffer containing 300 mM NaCl to stabilize DNA duplexes. In relatively short time (<1 h), the aggregates would sink to the bottom of the container due to gravity. Therefore, the aggregates can be considered to be separated from the solution phase. The research goal is to investigate Pb^{2+} -induced disassembly of the aggregates.

(33) Chen, S. *Adv. Mater.* **2000**, *12*, 186–189.

(34) Chang, J.-Y.; Wu, H.; Chen, H.; Ling, Y.-C.; Tan, W. *Chem. Commun.* **2005**, 1092–1094.

(35) Liu, X.; Theil, E. C. *Acc. Chem. Res.* **2005**, *38*, 167–175.

(36) Hazarika, P.; Ceyhan, B.; Niemeyer, C. M. *Angew. Chem., Int. Ed.* **2004**, *43*, 6469–6471.

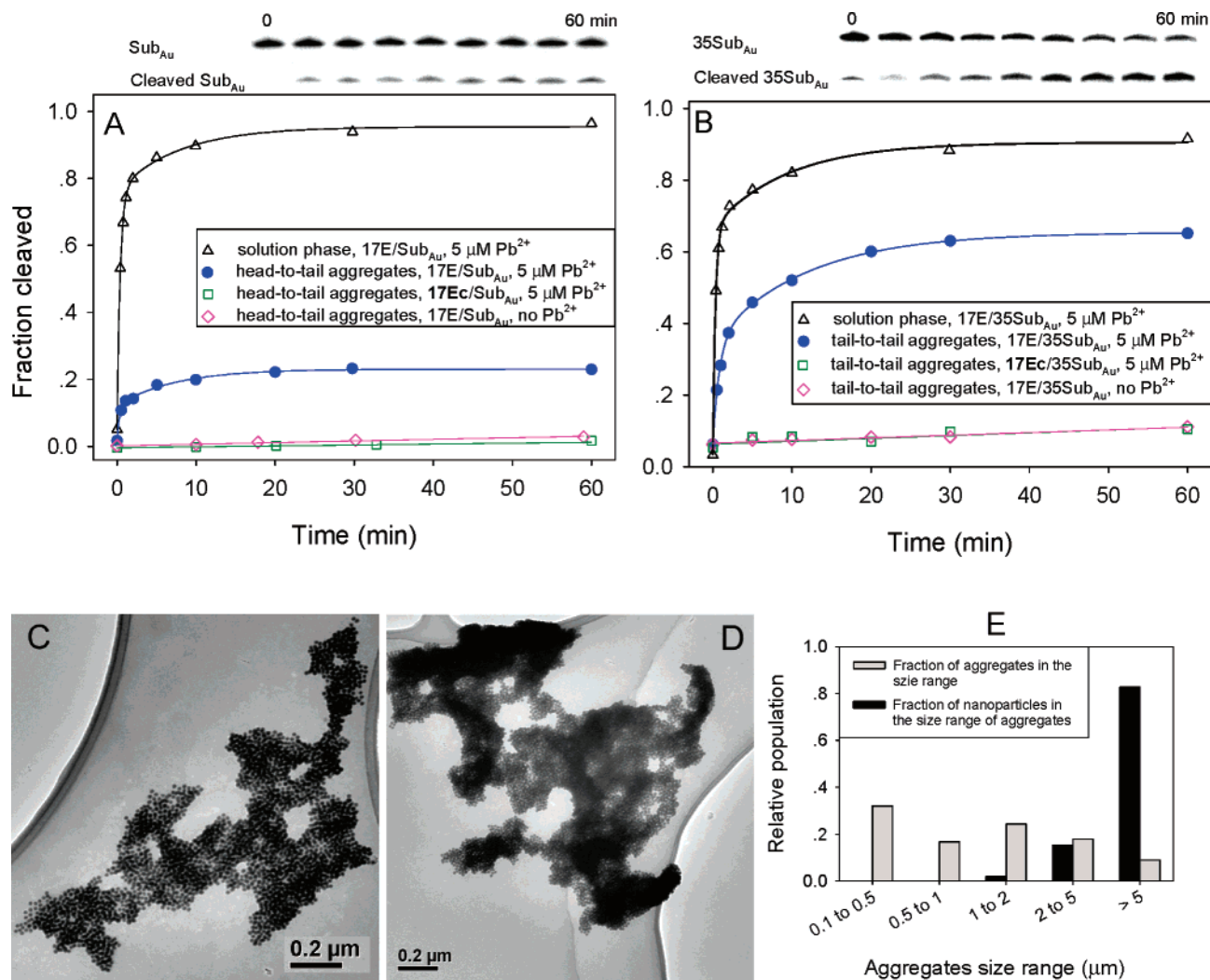


Figure 2. Activity assays performed with ³²P-labeled substrate for the head-to-tail (A) and tail-to-tail (B) aligned aggregates. The solution phase reactions were carried out with 3 μM of enzyme (17E) and ~1 nM substrate (Sub_{Au} or 35Sub_{Au}). The radioautograph shown in each panel corresponds to the curve show in blue. (C, D) Two typical TEM images of tail-to-tail aligned aggregates assembled by 17E and 35Sub_{Au}. Images were acquired on a JOEL 2010 TEM. (E) Size distribution of nanoparticle aggregates (gray bars) and the fraction of the number of nanoparticles in each size range (black bars). (A total of 78 aggregates were analyzed.)

Biochemical Assays in Nanoparticle Aggregates. To study Pb²⁺-induced disassembly, Pb²⁺ was added to the aggregate suspensions. However, no disassembly or color change was observed for either head-to-tail or tail-to-tail aligned aggregates. The failure to observe color change could be attributed to two possible reasons. First, by confining the DNAzyme in nanoparticle aggregates, its cleavage activity was inhibited. Second, the enzyme was active, but the release of cleaved substrate fragments and nanoparticles from the aggregates was inhibited, and nanoparticles were still assembled by cleaved substrate pieces (vide infra).

To investigate whether the DNAzyme was active when embedded in aggregates, the substrate strands of the DNAzyme were labeled with ³²P at the 5'-ends (label Sub_{Au} for the head-to-tail and 35Sub_{Au} for the tail-to-tail alignment, see Table 1 for DNA sequences), and the ³²P-labeled substrates were used to assemble nanoparticles. After addition of Pb²⁺ to the aggregate suspensions, the reaction kinetics were followed by standard biochemical assay procedures.³¹ The cleaved and uncleaved substrates were separated by gel electrophoresis. Shown in Figure 2A is a radioautograph of the cleavage kinetics

of head-to-tail aligned aggregates. The upper band is the uncleaved substrate (Sub_{Au}), and the lower band is the cleaved Sub_{Au}. The fraction of cleavage was quantified as shown in the plot below (blue dots). Initially, the reaction was fast. After reaching a plateau of 22% cleavage in ~10 min, no further cleavage was observed in 1 h. In comparison, 60% cleavage was observed for tail-to-tail aligned aggregates (Figure 2B).

To confirm that the cleavage was truly due to the Pb²⁺-activated DNAzyme, several control experiments were performed. First, if no Pb²⁺ was added, no cleavage was observed (pink diamonds), suggesting that Pb²⁺ was required for cleavage. Second, it is known that by mutating the G-T wobble pair in the DNAzyme to a G-C Watson-Crick base pair, the activity of the DNAzyme is abolished.³¹ The mutated enzyme strand is named 17Ec (Figure 1A). If aggregates were prepared with 17Ec instead of 17E, even in the presence of Pb²⁺, no cleavage was observed (green squares), suggesting that the cleavage was indeed catalyzed by the DNAzyme. Under the same reaction condition, single turnover solution phase reactions were also carried out for comparison. In both cases, more than 90% cleavage was observed (Figure 2A,B, triangles). From the

Table 1. Names and Sequences of DNA Used in the Work^a

Name	Sequence (listed from 5'-end to 3'-end)
17E	CATCTCTTCTCCGAGCCGGTCGAAATAGTGAGT
17Ec	CATCTCTTCCCCGAGCCGGTCGAAATAGTGAGT
35Sub _{Au}	ACTCATCTGTGAACTACTATr AGGAAGAGATGTGTCAACTCGTG
Inva	CACGAGTTGACACATCTCTTCC TATAGTGAGTTCACAGATGAGT
Inva-2	CGAGTTGACACATCTCTTCC TATAGTGAGTTCACAGATGA
Inva-4	AGTTGACACATCTCTTCC TATAGTGAGTTCACAGAT
Inva-6	TTGACACATCTCTTCC TATAGTGAGTTCACAG
Inva-8	GACACATCTCTTCC TATAGTGAGTTCAC
Sub _{Au}	TGTCAACTCGTGACTACTATr AGGAAGAGATGTGTCAACTCGTG
HT_Inva	CACGAGTTGACACATCTCTTCC TATAGTGAGTTCACGAGTTGACA
5'DNA _{Au}	Au nanoparticle-S-(CH ₂) ₆ -CACGAGTTGACA
3'DNA _{Au}	TCACAGATGAGT-(CH ₂) ₃ -S-Au nanoparticle
rA (in bold face) represents the ribo-adenosine (cleavage site)	

^a Under each name of invasive DNA, there are two DNA strands, complementary to the two cleaved substrate pieces, respectively (i.e., 2 μ M Inva-6 means 2 μ M for each strand).

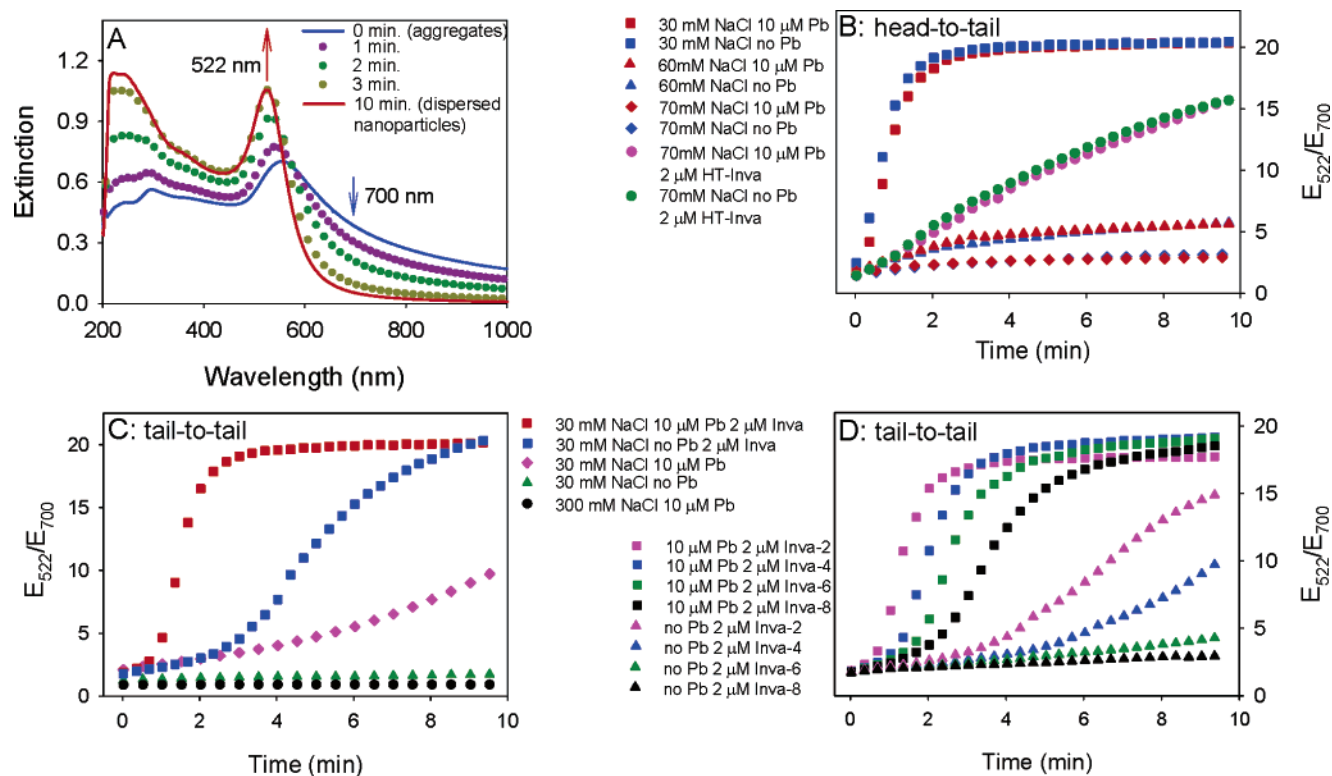


Figure 3. (A) Time-dependent UV-vis spectra of tail-to-tail aligned aggregates in the presence of 5 μ M Pb²⁺ and 2 μ M Inva-6. After 10 min, all nanoparticles were disassembled into solution with a high extinction ratio (522 over 700 nm) obtained. Comparison of disassembly kinetics in the presence and absence of Pb²⁺ for head-to-tail (B) and tail-to-tail (C) aligned aggregates. (D) Comparison of disassembly kinetics in the presence of different invasive DNA for tail-to-tail aligned aggregates in 30 mM NaCl.

results, it appeared that the DNAzyme was active in both aggregates, and the problem was the release of nanoparticles after cleavage.

Disassembly Aided by Decreasing NaCl Concentration. Nanoparticles were assembled by DNA base-pairing interactions. To facilitate the release of nanoparticles, the NaCl concentration was decreased, because NaCl is known to stabilize DNA duplexes. The process of disassembly was monitored with UV-vis spectroscopy. Dispersed 13-nm nanoparticles have a strong extinction peak at 522 nm (Figure 3A, red curve). Upon aggregation, the 522-nm peak decreases, while the extinction in the 700-nm region increases (Figure 3A, blue curve). Therefore, the ratio of extinction at 522 and 700 nm was used to characterize the assembly state of nanoparticles. Dispersed

nanoparticles have a high extinction ratio and a red color, while aggregated nanoparticles have a low ratio and a blue color. Pb²⁺ was added to the aggregate suspensions to test whether the rate of disassembly would increase. For the head-to-tail aligned aggregates, however, no difference was observed in the presence or absence of Pb²⁺ even in low NaCl concentration buffers (70, 60, and 30 mM) (Figure 3B, red and blue curves). Further decrease of NaCl would render very low stability of the aggregates and was not investigated.

The tail-to-tail aligned aggregates were more stable in low NaCl concentration buffers. For example, the aggregates were stable for more than 10 min in 30 mM NaCl (Figure 3C, green triangles). Interestingly, when Pb²⁺ was added to tail-to-tail aligned aggregates suspended in 30 mM NaCl, a slow color

change was observed (Figure 3C, pink diamonds). However, the color change or the disassembly was inhibited in high salt buffers (i.e., 300 mM NaCl, Figure 3C, black dots). These results confirmed that the DNAzyme was active in tail-to-tail aligned aggregates. With high salt buffers, the release of nanoparticles from cleaved substrate pieces was inhibited. After cleavage, the substrate (35Sub_{Au}) was broken into two pieces of equal length (22 nucleotides each). Twelve bases of the 22-mer were hybridized to the DNA attached to nanoparticles; nine were complementary to the enzyme strand, with one overhang left. It was believed that, in high salt buffers, the release of the cleaved substrate pieces from the nine base pairs formed with the enzyme was inhibited. Therefore, nanoparticles could still be linked by the cleaved substrate, as schematically represented in Figure 1F (highlighted with a red circle).

Disassembly Aided by Invasive DNA. Although disassembly of nanoparticles was observed for the tail-to-tail aligned aggregates by decreasing NaCl to 30 mM, the rate of disassembly was relatively slow. Further decrease of NaCl could not be used to accelerate the releasing step, as aggregates became unstable. The disassembly of nanoparticle aggregates should be an entropy-favored process. To compensate for the energy loss of the process and to make it enthalpy-favored, two 22-mer DNA (called invasive DNA) that were complementary to the cleaved substrate were added to help release the cleaved substrate. It was observed that the disassembly was close to completion in 2 min in the presence of 10 μ M of Pb²⁺ and 2 μ M of the invasive DNA (Figure 3C, red squares). However, the background disassembly in the absence of Pb²⁺ also went up significantly (Figure 3C, blue squares). This result can be attributed to the invasive DNA invading not only cleaved substrate, but also uncleaved substrate at a significant rate. To suppress the background disassembly, a series of shorter invasive DNA with a reduced number of base pairs to the two ends of the uncleaved substrate were tested (named Inva-2, Inva-4, Inva-6, and Inva-8; see Table 1). These invasive DNA should target more specifically toward cleaved substrates than for uncleaved ones. Indeed, as observed from Figure 3D, the background disassembly (in the absence of Pb²⁺) was suppressed with shorter invasive DNA, although the rate of disassembly in the presence of Pb²⁺ decreased slightly too. As a compromise between the rate of disassembly and the level of background, Inva-6 was chosen for further assays of the system.

The invasive DNA approach was also applied to the head-to-tail aligned aggregates. However, still no difference was observed for samples with or without added Pb²⁺ (Figure 3B, pink and green dots). The results led us to reconsider the origin of the 22% cleavage observed for head-to-tail aligned aggregates (Figure 2A, blue dots). DNAzymes attached to nanoparticles can be classified into two populations. The first population is the cross-linking DNAzymes that link to two nanoparticles and is responsible for the aggregation. The second population is the dangling DNAzymes that attach by only one end to a nanoparticle, while leave the other end free. The dangling DNAzymes on nanoparticles had been largely ignored thus far. The fact that no Pb²⁺-dependent disassembly could be detected suggested that the 22% cleavage observed for the head-to-tail aggregates was from dangling DNAzymes and that cross-linking DNAzymes were inactive. The length of a 44-mer (length of the substrates) B-form DNA duplex is \sim 15 nm. It is likely that, for the head-

to-tail alignment, the steric hindrance of nanoparticles (13-nm diameter) posed on the DNAzyme is much higher than that in the tail-to-tail alignment.

Disassembly of Nanoparticle Aggregates as a “Light-Up” Colorimetric Sensor. After demonstrating the controlled disassembly of gold nanoparticle aggregates in response to Pb²⁺, we tested the potential of using the tail-to-tail aligned aggregates as a “light-up” colorimetric sensor for Pb²⁺. Shown in Figure 3A is a time-dependent UV–vis spectra evolution of the aggregates in the presence of 5 μ M of Pb²⁺ and 2 μ M of Inva-6. An increase of 522 nm and a decrease of 700-nm extinction were observed. The same experiment was repeated with different Pb²⁺ concentrations and different metal ions. As shown in Figure 4A, the rate of disassembly increased with increasing Pb²⁺. For simple quantification, the extinction ratios at 5 min after initiation of disassembly were plotted versus Pb²⁺ concentrations (Figure 4B, red dots), from which Pb²⁺ could be quantified from 0.1 to 2 μ M. In a control experiment, when the inactive mutant (17Ec, see Figure 1A) was used instead of 17E to assemble nanoparticles, no Pb²⁺-dependent disassembly was observed and the color remained blue (Figure 4B, blue squares). For metal specificity, although nanoparticles were attached, the catalytic core of the DNAzyme was not modified, and the high selectivity for Pb²⁺ of the DNAzyme should be maintained. Indeed, as shown in Figure 4C, with 5 μ M of different divalent metal ions, only Pb²⁺ induced fast disassembly. By spotting the sensor solution with different added metal ions on a solid substrate (i.e., an alumina TLC plate), the displayed color could be conveniently compared (Figure 4D). With increasing Pb²⁺, color progression from blue to purple to red was observed, while other metal ions gave only background blue color. Therefore, this system was capable of detecting Pb²⁺ at room temperature in 5 min with high sensitivity and selectivity.

Although the work was performed with a Pb²⁺-specific DNAzyme, there are many other stimuli-responsive DNAzymes,^{19–24} RNAzymes (ribozymes),^{37,38} effector-regulated nucleic acid enzymes (aptazymes),^{39–43} and aptamers.^{44,45} By incorporating nanoparticles into those functional nucleic acids, a diverse range of functional nanomaterials can be obtained to sense a broad range of analytes. However, before these applications can be generally realized, at least two important factors should be considered. First, it is important to fine-tune the interaction between DNAzymes and nanoparticles. For example, only the tail-to-tail construct worked, but not the head-to-tail alignment. This difference is attributable to large steric hindrance of the head-to-tail alignment toward the DNAzyme active site, affecting efficient enzymatic cleavage and thus disassembly. However, the exact origin of this difference is still not clear and will be addressed in future studies. Second, the DNAzyme-assembled nanoparticle aggregates disassembled most efficiently in low salt buffers (e.g., 30 mM NaCl for tail-to-tail aligned aggregates), which may pose stability issues for practical applications of the material. Synthesis of nanomaterials that can

(37) Cech, T. R. *Biochem. Soc. Trans.* **2002**, *30*, 1162–1166.

(38) DeRose, V. J. *Chem. Biol.* **2002**, *9*, 961–969.

(39) Soukup, G. A.; Breaker, R. R. *Curr. Opin. Struct. Biol.* **2000**, *10*, 318–325.

(40) Tang, J.; Breaker, R. R. *Chem. Biol.* **1997**, *4*, 453–459.

(41) Breaker, R. R. *Curr. Opin. Biotechnol.* **2002**, *13*, 31–39.

(42) Wang, D. Y.; Lai, B. H. Y.; Sen, D. J. *Mol. Biol.* **2002**, *318*, 33–43.

(43) Achenbach, J. C.; Nutiu, R.; Li, Y. *Anal. Chim. Acta* **2005**, *534*, 41–51.

(44) Ellington, A. D.; Szostak, J. W. *Nature* **1990**, *346*, 818–822.

(45) Famulok, M.; Mayer, G.; Blind, M. *Acc. Chem. Res.* **2000**, *33*, 591–599.

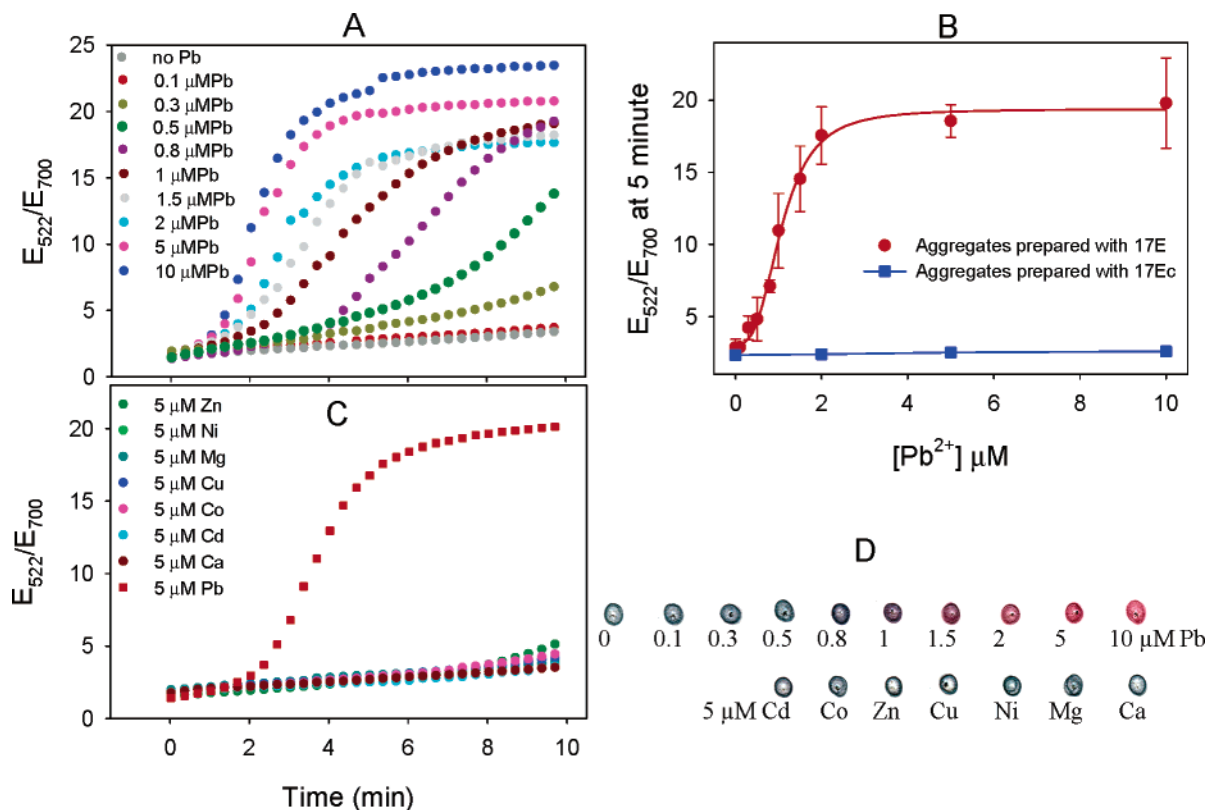


Figure 4. (A) Kinetics of disassembly in the presence of different Pb^{2+} concentrations. All samples contained $2 \mu\text{M}$ of Inva-6 and 30 mM NaCl. (B) Extinction ratios after disassembly for 5 min for aggregates with different Pb^{2+} concentrations. (C) Kinetics of disassembly in the presence of $5 \mu\text{M}$ of Pb^{2+} or other divalent metal ions. (D) Color developed on an alumina TLC plate after 5 min of disassembly.

disassemble in a wider salt concentration range will be another direction for future studies.

Conclusions

We have demonstrated chemical stimuli-responsive disassembly of nanoparticle aggregates using Pb^{2+} -specific DNAzymes. By simple switching of nanoparticle alignment, these similar aggregates had drastically different properties. A better understanding of the system at nanoscale has improved the colorimetric Pb^{2+} sensor from “light-down” to “light-up”. DNA has well-defined and predictable structures, combined with the various biological activities of DNAzymes and the optical properties of metallic nanoparticles. The DNAzyme/nanoparticle system offers us an ideal model system to study the interaction of nanoparticles with biomolecules at nanoscale.

Experimental Section

Materials and Nanoparticle Aggregates Preparation. All DNA samples were purchased from Integrated DNA Technologies Inc. The substrate and enzyme DNA were purified by HPLC by the company, and all other DNA were purified by standard desalting. Gold nanoparticles (13-nm diameter) were prepared following literature procedures.^{46,47} Thiol-modified DNA (1 mM) was activated with TCEP (2 mM) for 1 h before attaching to gold nanoparticles. Other procedures of attaching followed published methods.⁴⁷ To prepare tail-to-tail aligned aggregates, a solution was prepared to contain 6 nM $3'\text{DNA}_{\text{Au}}$, 6 nM $5'\text{DNA}_{\text{Au}}$, 400 nM 17E, 100 nM 35Sub_{Au}, 300 mM NaCl, and 25 mM

Tris acetate buffer, pH 8.2. The final extinction at 522 nm was ~ 2.2 . The mixture was warmed to $60 \text{ }^\circ\text{C}$ for 3 min and allowed to cool slowly to room temperature in 4 h in a water bath. After brief centrifugation, dark purple nanoparticle aggregates precipitated to the bottom. The supernatant was removed, and the aggregates were washed three times with a buffer containing 100 mM NaCl and 25 mM Tris acetate, pH 8.2, and were finally suspended in the same buffer. The concentration was adjusted so that after 9 times dilution and after complete disassembly into dispersed nanoparticles, the extinction at 522 nm was ~ 1 . The suspended aggregates were then stored in a $-20 \text{ }^\circ\text{C}$ freezer and were thawed at room temperature before use. To prepare head-to-tail aggregates, the procedures were similar, except that 12 nM $5'\text{DNA}_{\text{Au}}$ (no $3'\text{DNA}_{\text{Au}}$) was used and the substrate was Sub_{Au}. NaCl concentration was 400 mM for the preparation and 300 mM for washing and storage. To prepare aggregates containing ^{32}P -labeled substrate, $\sim 0.1\%$ of ^{32}P -labeled substrates (in respect to the total substrate amount) was added, while keeping other conditions the same. For control experiments, 17E was used instead of 17E to assemble nanoparticles, while other procedures were the same.

Activity Assays. ^{32}P -Labeled aggregates were added to a solution with $5 \mu\text{M}$ Pb^{2+} , 300 mM NaCl, and 25 mM Tris acetate, pH 8.2. Aliquots were taken out at designated time points and quenched in a solution containing 8 M urea and 200 mM EDTA. The quenched aliquots were heated at $60 \text{ }^\circ\text{C}$ to fully release substrate strands from aggregates and then loaded to 20% denaturing polyacrylamide gel. ^{32}P -Labeling and procedures for single-turnover solution phase activity assays were the same as reported elsewhere.^{30,31}

Disassembly Kinetics Monitoring. The kinetics of disassembly was monitored on a Hewlett-Packard 8453 spectrophotometer operating in the kinetics mode. All reagents except nanoparticle aggregates were added into a quartz cell with a final volume of $80 \mu\text{L}$, and a blank spectrum was taken. The disassembly was initiated by adding $10 \mu\text{L}$ of aggregates. The dead time between adding aggregates to collecting

(46) Grabar, K. C.; Freeman, R. G.; Hommer, M. B.; Natan, M. J. *Anal. Chem.* **1995**, *67*, 735–743.

(47) Storhoff, J. J.; Elghanian, R.; Mucic, R. C.; Mirkin, C. A.; Letsinger, R. L. *J. Am. Chem. Soc.* **1998**, *120*, 1959–1964.

the first spectrum was controlled to be ~ 10 s. The mixture was agitated at least every minute to prevent precipitation of the aggregates. In some cases, 10 μL of the mixture was taken out and spotted on a TLC plate. After drying, the TLC plate was scanned with a conventional scanner to acquire images (Canon 5000F).

Acknowledgment. We are grateful for the funding of this research by the U.S. Department of Defense through the

Multidisciplinary University Research Initiative (MURI) Program, by the National Science Foundation through a Science and Technology Center of Advanced Materials for Purification of Water with Systems (WaterCAMPWS), and by the Illinois Waste Management and Research Center.

JA053567U